Nucleic Acids Research, 2005, Vol. 33, No. 5 ***1487–1502***
doi:10.1093/nar/gki290

Characterizing the function and structural organization of the 5′ tRNA-like motif within the hepatitis C virus quasispecies

Maria Piron[1], Nerea Beguiristain[1], Anna Nadal[1], Encarnación Martínez-Salas[2] and Jordi Gómez[1,3,*]

[1]Servicio de Medicina Interna-Hepatología, Edifici de Recerca, Hospital Vall d'Hebron, Paseo Vall d'Hebron 119-129, Barcelona 08035, Spain, [2]Centro de Biología Molecular Severo Ochoa, CSIC-UAM, Cantoblanco, 28049 Madrid, Spain and [3]Centro de Investigación en Sanidad Animal, INIA, Valdeolmos, 28130 Madrid, Spain

Received November 24, 2004; Revised and Accepted February 18, 2005 EMBL/DDBJ/GenBank accession nos AY576547–AY576603

ABSTRACT

Hepatitis C virus (HCV) RNA is recognized and cleaved *in vitro* by RNase P enzyme near the AUG start codon. Because RNase P identifies transfer RNA (tRNA) precursors, it has been proposed that HCV RNA adopts structural similarities to tRNA. Here, we present experimental evidence of RNase P sensitivity conservation in natural RNA variant sequences, including a mutant sequence (A368–G) selected *in vitro* because it presented changes in the RNA structure of the relevant motif. The variation did not abrogate the original RNase P cleavage, but instead, it allowed a second cleavage at least 10 times more efficient, 4 nt downstream from the original one. The minimal RNA fragment that confers sensitivity to human RNase P enzyme was located between positions 299 and 408 (110 nt). Therefore, most of the tRNA-like domain resides within the viral internal ribosome entry site (IRES) element. In the variant, in which the mutation stabilizes a 4 nt stem–loop, the second cleavage required a shorter (60 nt) substrate, internal to the minimal fragment substrate, conforming a second tRNA-like structure with similarities to a 'Russian-doll' toy. This new structure did not impair IRES activity, albeit slightly reduced the efficiency of translation both *in vitro* and in transfected cells. Conservation of the original tRNA-like conformation together with preservation of IRES activity points to an essential role for this motif. This conservation is compatible with the presence of RNA structures with different complexity around the AUG start codon within a single viral population (quasispecies).

INTRODUCTION

Hepatitis C virus (HCV) genome consists of a single-stranded RNA of approximately 9600 nt in length with a plus polarity. Sequence analysis of a large number of complementary DNA (cDNA) clones of HCV from single isolates has provided evidence that the HCV genome cannot be defined by a single sequence, but rather by a population of variant sequences closely related to one another (1). This manner of organizing the genetic information, which characterizes most RNA viruses, is called quasispecies (2). It is theoretically predicted that, after RNA folding, part of the variability present in the RNA sequences of the viral population may still be represented in secondary or tertiary RNA structures, providing alternative conformations (3). This variability could potentially modify the strength of RNA conformational signals, which represent potential substrates for selection events, or provide the signals with different meanings. Nevertheless, the predictable phenomenon related to RNA structural variability in viral quasispecies has not been extensively evaluated experimentally, probably because it is difficult to identify variant structures among very similar sequences.

HCV RNA comprises a 5′ untranslated region that functions as an internal ribosome entry site (IRES, Figure 1). The highly structured IRES comprises most of the 5′ untranslated sequence (4) and extends in the AUG downstream sequence, possibly including 30 nt of the core coding sequence (5–8). Although the exact 3′ boundary of the HCV IRES is subjected to controversy, it is clear that the activity of the IRES can be profoundly influenced by the nature of the immediate downstream coding sequences [(reviewed in (9)].

In a previous work, we identified two positions within the viral genome that were cleaved *in vitro* specifically by human RNase P, the enzyme that processes tRNA precursors (pre-tRNA) (10). One of the susceptible positions is located at the 3′ vicinity of the initiator AUG codon (Figure 1). Recently, it was

*To whom correspondence should be addressed. Tel: +1 34 93 489 40 34; Fax: +1 34 93 489 40 32; Email: jgomez@vhebron.net

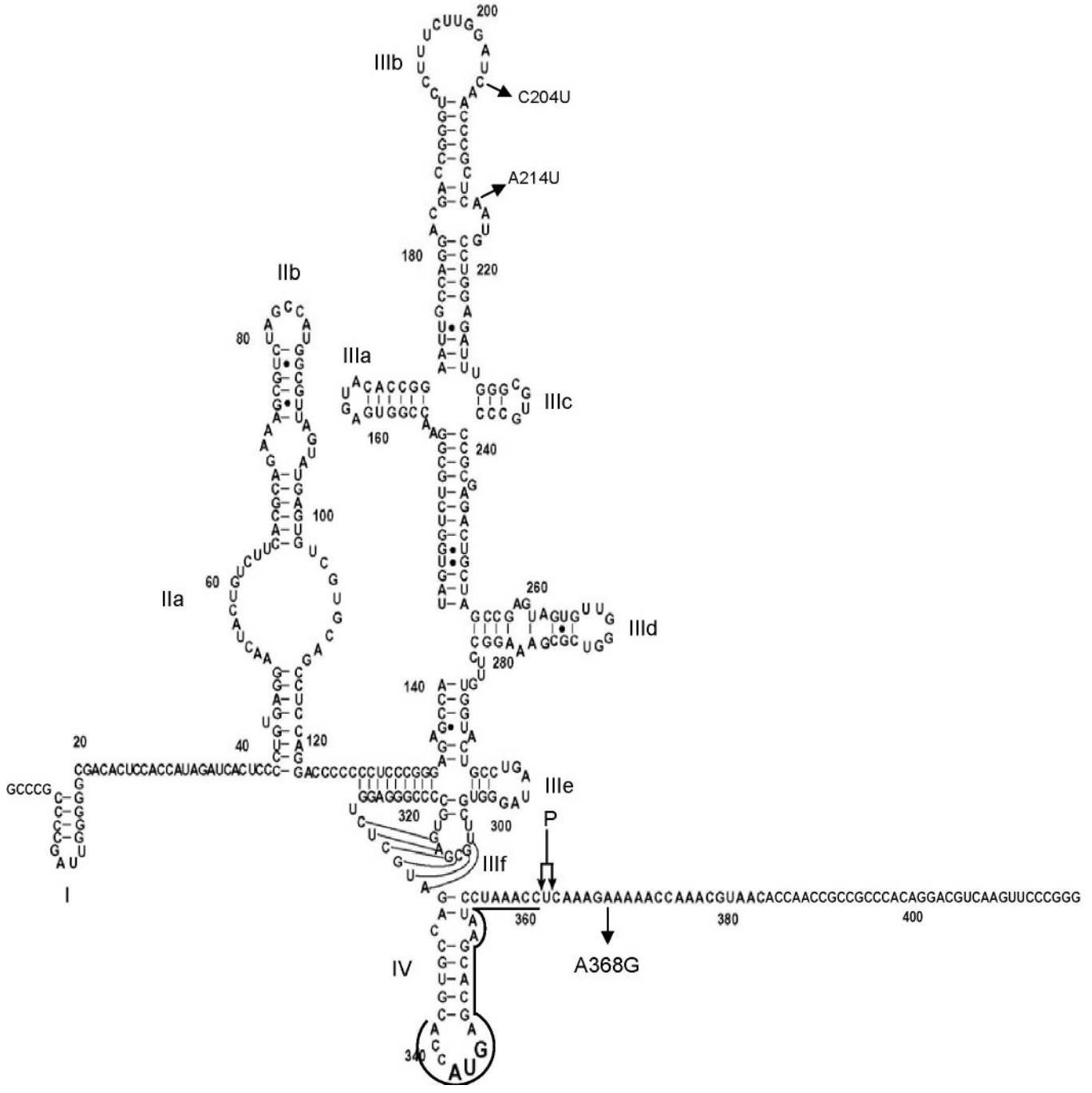

Figure 1. Diagram of genotype 1b HCV IRES RNA secondary structure (sequence 2–418 used in this work) modified from (25). Substitutions C204U and A214U in the WT sequence are indicated; the A368G sequence only differs from the WT sequence by the A368G mutation. A double arrow indicates RNase P cleavage site (361–363). A line between nucleotides 339 and 361 depicts the hybridization site of a DNA primer used for *in vitro* selection in Figure 2. Structural sub-domains are indicated from I to IV.

shown that the catalytic RNA from RNase P of *Synechocystis* sp. also cleaved specifically at the 5′ vicinity of the AUG codon (11). RNase P cleavage is not a unique property of the HCV genome. Cleavage by human RNase P has been mapped in a similar position near the AUG of the related animal pestiviruses, CSFV (classical swine fever virus) and BVDV (bovine viral diarrhea virus), and has been detected near the initiation codon of other unrelated RNA virus families (12).

Substrate recognition by RNase P is structure dependent (13). RNase P cleavage has reliably identified a number of authentic tRNA-like domains in non-tRNA molecules, including bacterial SRP (signal recognition particle) RNA and tmRNA (transfer-messenger RNA), and various plant viral RNA genomes (14–18). Recognition of HCV RNA by the RNase P enzyme and the ability of HCV RNA to compete with pre-tRNA processing by this enzyme have led to propose that viral RNA adopts internally a structural motif similar to

the tRNA molecule (10–12). Although the function of the tRNA-like structures found in HCV RNA is unknown (10), the proximity of one of the RNase P substrates to the AUG suggests that it may have a role in the initiation of viral RNA translation, probably by recruiting small ribosomal subunits (12). In fact, HCV IRES does not require all the canonical initiation factors to recruit the ribosome, and is able to directly bind the 40S subunit (19,20). Various studies have pointed out the importance of stable independent structural RNA domains in the IRES for ribosome recruitment (19,21–23). Furthermore, it has been shown that this interaction, as well as the HCV IRES RNA structure, is magnesium dependent (19,24).

With this in view, we have made efforts to characterize the minimal tRNA-like domain, and indirectly assess its relevance within the viral life cycle, by measuring its degree of conservation either in different patients or in a single patient quasispecies, as well as its effect in IRES-dependent translation.

In this study, we used human RNase P enzyme as a tool to study the tRNA-like motif located near the translation initiation codon of HCV RNA. We characterized this structural motif using a population-based approach, as would be defined by a population geneticist. The reason was that the population of HCV RNA molecules is highly variable and that variability in the primary structure may be expressed in the final conformation RNA adopts. The analysis was conducted along three consecutive phases: in the first, we analyzed the sequence composition of the viral population of sequences around the AUG codon in several patients and assayed the RNase P enzyme accessibility in the variant RNAs. In the second, we selected *in vitro* a conformational variant from a population of sequences from a single patient; in the third, we characterized the tRNA-like domain of the conformational variant and of the most frequently represented sequence in the total population. Characterization included the following comparative studies: (i) *in vitro* sensitivity to RNase P; (ii) minimal fragment length requirement and localization in the viral genome; (iii) secondary RNA structure probing; and (iv) *in vitro* and in cell culture efficiency of internal initiation of translation. Direct analysis of RNA integrity showed that the HCV RNA is not accessible to RNase P in the cytoplasm of transfected cells, strongly suggesting that this conserved tRNA-like motif may provide a signal for HCV RNA life cycle, different from RNA processing.

MATERIALS AND METHODS

Clinical and virological characteristics of the HCV infected patients in the study

We selected eight patients infected with hepatitis C virus at different stages of the disease. One (Patient 1) was in the acute phase of the disease. The others were chronically infected, one (Patient 2) with mild, two (Patients 3 and 4) with moderate and, and three (Patients 5, 6 and 7) with severe liver damage. The last one (Patient 8) presented liver cirrhosis. Viral loads ranged from 10^5 genome copies/milliliter in patient 2, to 10^7 copies/milliliter in patient 1. No one has been previously treated and they were not co-infected with other hepatitis virus or human immunodeficiency virus.

RNA extraction, RT–PCR, cloning and sequencing

Viral RNA was extracted from serum samples (140 μl) from HCV-infected patients (Patients 1–8) with the QIAamp viral RNA mini kit (Qiagen). Isolated HCV RNA was reverse-transcribed into cDNA, with a genotype 1b-specific primer from the IRES-core region (CORE 419(−) 5′-CCACCAACGATCTGACCACCG), and nested PCR was then performed to obtain the 2–418 fragment [outer set: 5′-2(+) 5′-CGCGGATCCGGCCGCCCCGATTGGGGGCGA and CORE 419(−) inner set 5′ T7-2(+)CGCGGATCCTAATACGACTTAATACGACTCACTATAGGCCGCCCCGATTGGGGGCGA (BamHI cloning site underlined) and CORE 394(−) 5′-CCGGAATTCCCCGGGAACTTGACGTCCTGTGGGC (EcoRI cloning site underlined)].

T7-HCV 2–418 DNA molecules were cloned in a pUC18 vector between the BamHI and EcoRI restriction sites and transformed in the *Escherichia coli* DH5α strain. Individual clones were sequenced by the dideoxy chain terminator method with the DNA sequencing kit (ABI PRISM dRhodamine Terminator Cycle Sequencing Ready Reaction kit, Applied Biosystems) using M13 and reverse M13 primers and analyzed in an ABI PRISM 310 Genetic Analyzer (Applied Biosystems).

We performed an analysis of the sequence composition of the viral quasispecies of the 5′ NCR-core junction region, around the 5′ RNase P cleavage site (361–363), from positions 23 to 393. A total of 155 HCV cDNA clones were sequenced from the eight infected patients described before. Sequences were then compared and the predominant and mutant sequences were identified for each patient.

In vitro selection

Step 1: We started with the HCV RNA viral sequence population extracted, reverse-transcribed and amplified in serum from Patient 5. We obtained DNA fragments containing the phage T7 promoter sequence followed by DNA corresponding to positions 2–418 of the HCV genome (see previous section and Figure 2).

Step 2: Amplified HCV DNA 2–418 molecules were transcribed *in vitro* in the presence of [α-^{32}P]GTP, and the labeled RNA transcripts were polyacrylamide gel-purified and quantified in a scintillation counter (for more details see '*In vitro* transcription' section).

Step 3: The labeled RNA mixture was subjected to DNA-mediated RNase H cleavage using a DNA oligonucleotide complementary to nucleotides 339–361 of HCV RNA. With this preliminary kinetic experiment, we determined the incubation time of the reaction that released 50% of the product bands.

Step 4: Once the experimental conditions to cleave 50% of RNA transcripts had been determined, a preparative experiment was performed and non-cleaved RNAs were gel excised, eluted from gel and ethanol precipitated. They were quantified and again subjected to RT–PCR, which began a new selection cycle.

Four selection cycles were performed. DNA fragments obtained after step 1 were cloned in *E.coli* and 20 clones were sequenced after cycles 0, 2 and 4.

Obtaining shorter HCV DNA templates for transcription

In order to define the RNase P minimal sequence length requirement, nine shorter DNA templates were consecutively

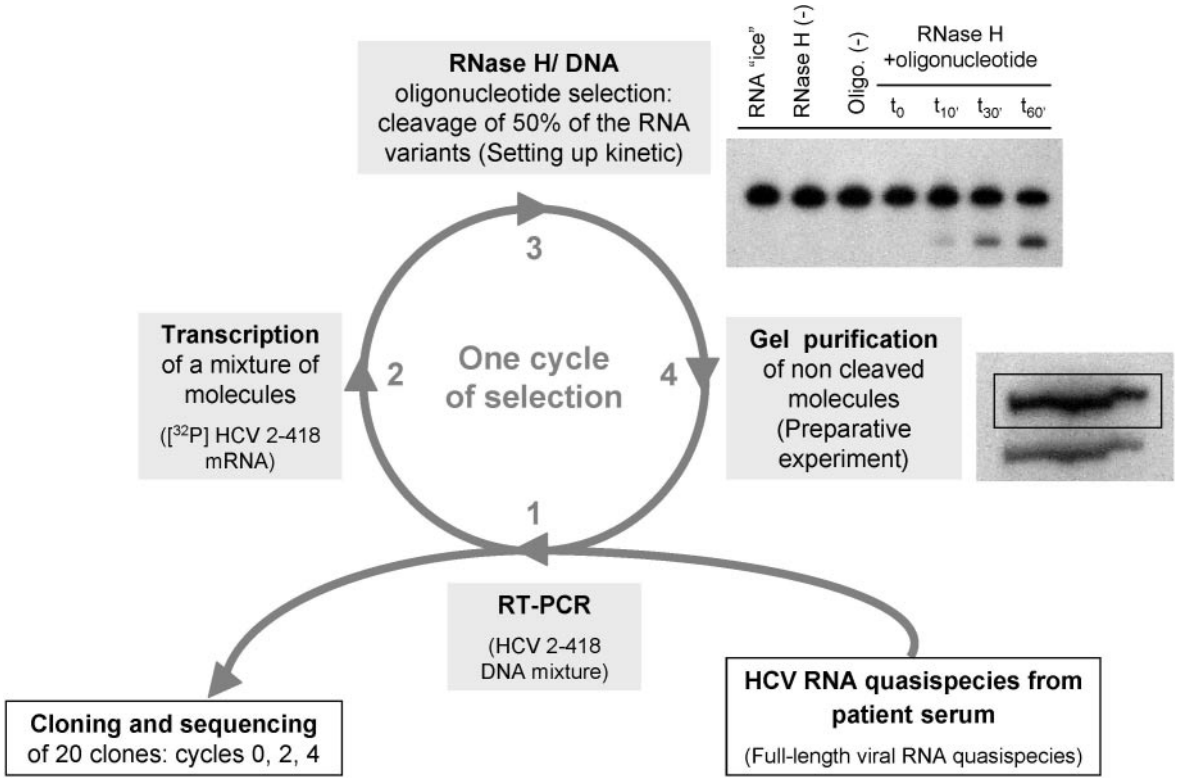

Figure 2. Schematic representation of *in vitro* selection procedure for isolating natural HCV IRES RNA structure variants using RNase H/DNA oligonucleotide-mediated cleavage of HCV mRNA. See Materials and Methods for details.

obtained by PCR from pUC18 containing HCV nucleotides 2–418 (WT and A368G). The oligonucleotide sequences used were 5′T7 291(+): 5′-TAATACGACTCACTATAGGGC-CATGGCCTGATAGGGTGCTTGCGA (G291 underlined); 5′T7 299(+): 5′-TAATACGACTCACTATAGGGTGCTTG-CGAGTGCCCCG; 5′T7 311(+): 5′-TAATACGACTCAC-TATAGGTGCCCCGGGAGGTCTCGTAG; 5′T7 331(+): 5′-TAATACGACTCACTATAGACCGTGCACCATGAGC-ACG; CORE T7 350(+): 5′-TAATACGACTCACTATA-GAATCCTAAACCTCAAAGGA; CORE 418(−): 5′-CCG-GAATTCCCCGGGAACTTGACGTCCTGTGGGC^{394} (418 position underlined); CORE 408(−): 5′-^{408}TGACGTCC-TGACGTCCTGTGGGCGGCGG^{389}; CORE 398(−): 5′-^{398}TGGGCGGCGGTTGGTGTTAC^{379}; CORE 390(−): 5′-^{390}GGTTGGTGTTACGTTTGGTTTT^{369}; CORE 380mut(−): 5′-^{380}ACGTTTGGTTTTCCTTTGAGG^{360} (A368G mutation underlined).

In vitro transcription

RNA transcripts were obtained from the PCR DNA mixture (*in vitro* selection procedure), from EcoRI (2–418 HCV) or FokI (pUC19TyrT) linearized plasmids, or from the PCR products.

Transcription reactions were carried out as previously described (10). Briefly, 1 µg DNA template was transcribed *in vitro* (37°C, 1 h) with [α-^{32}P]GTP or [α-^{32}P]ATP followed by 5 min of treatment with RNase-free DNase I at 37°C. Cellulose CF11 chromatography was used to eliminate DNA fragments and non-incorporated nucleotides. Transcripts were then purified by gel electrophoresis under denaturing conditions on 4% polyacrylamide gels containing 7 M urea. Following X-ray film exposure, RNAs were excised from the gel and eluted in 10 mM Tris–HCl (pH 7.5) and 1 mM EDTA (pH 7.5). The concentration of radioactive transcripts was determined by calculating the amount of incorporated [α-^{32}P]GTP or [α-^{32}P]ATP based on scintillation counting.

For *in vitro* translation experiments, the HCV IRES predominant and A368G mutant 2–418 sequences were cloned in a bicistronic vector with the 26 first amino acids of HCV core protein fused in frame with the firefly luciferase. RNAs were obtained by *in vitro* transcription using T7 promoter and the MEGAscript high yield transcription kit (Ambion). RNA size was assessed by agarose gel electrophoresis and RNAs were quantified by trace radiolabeling.

RNA structure comparison between WT and A368G RNAs

DNA-directed RNase H cleavage. RNase H cleavage experiments were carried out according to a previously described method (25). The DNA primer complementary to HCV RNA 339–361 used in the *in vitro* selection experiment was 5′-GGGTTTAGGATTCGTGCTCATGGT. Purified RNA transcripts were resuspended at a concentration of 0.6 nM in the reaction mixture, DNA primer complementary to HCV IRES was added at a final concentration of 15 nM, with 250 ng carrier tRNA in 20 mM HEPES pH 8.0, 50 mM KCl, 10 mM $MgCl_2$ and 1 mM DTT, and finally, 0.5 U RNase H (Promega) was added in a final volume of 5 µl.

Reactions were incubated at 37°C from 0 to 90 min for kinetic experiments. Reactions were stopped by addition of 10 µl gel loading buffer and stored on ice. Reaction products were analyzed on denaturing 4% polyacrylamide gel containing 7 M urea and visualized by autoradiography.

RNase P cleavage. RNase P was previously purified in the laboratory from HeLa cells (10). RNA transcripts at a 1.8 nM final concentration were pre-heated for 1 min at 90°C before addition of reaction buffer (10 mM HEPES–KOH pH 7.5, 10 mM MgOAc, 100 mM NH4OAc) and left to cool for 20 min to room temperature. Cleavage reactions were performed for 30 min at 30°C in a final volume of 10 µl with 4% polyethylene glycol 8000, 20 U of RNase inhibitor RNasin (Promega) and 1 µl of RNase P peak activity. (pre)tRNA^{tyr} was used as substrate for human RNase P as positive control in some reactions.

Reaction products were electrophoresed on denaturing polyacrylamide gels containing 7 M urea and visualized by autoradiography.

For some experiments, RNase P cleavage efficiency was measured using a Radioisotopic Image Analyser FLA-5000 (Fuji). Quantitative data were obtained from triplicate experiments, average cleavage efficiency percentage was calculated as the ratio: products/products + uncleaved RNA.

RNA structure mapping with nucleases.
RNase T1 assays on uniformly labeled transcripts: Labeled RNA transcripts were mixed at a final concentration of 0.375 nM with 4 µg carrier tRNA in 10 mM HEPES–KOH (pH 7.5), 10 mM MgOAc, 100 mM NH_4OAc and 1 µg/µl (total cleavage) or 0.03 µg/µl (partial cleavage) RNase T1 was added in a final volume reaction of 20 µl. Reactions were incubated at 37°C, 20 min and analyzed on a denaturing 20% polyacrylamide gel containing 7 M urea. Results were visualized by autoradiography.

RNases T1, A and V1 assays on end-labeled transcripts: In order to obtain 3′ end-labeled transcripts, uniformly labeled and unlabeled 'cold' RNAs were both transcribed, run in parallel and bands were eluted from acrylamide gel. The 'cold' transcript was subsequently labeled with T4 RNA ligase and [^{32}P]pCp 5′ triphosphate under conditions similar to those described by the manufacturer. The reaction was carried out in 30 µl of 50 mM Tris–HCl pH 7.5, 10 mM $MgCl_2$, 10 mM DTT, 1 mM ATP, 0.01% BSA and 10% DMSO. The reaction mixture was incubated four days at 4°C. The labeled RNA was purified again using the electrophoretic procedure described above. For the 5′ end-labeled transcript preparations, 'cold' transcripts prepared as before were labeled with [α-^{32}P]GTP using the enzyme guanylyl transferase, and followed the same purification procedure.

For RNase reactions, the digestion mixture (10 µl) contained about 10^4 Cerenkov cpm of the 5′ or 3′ end-labeled transcript and 2.5 µg of carrier tRNA in 10 mM HEPES–KOH (pH 7.5), 10 mM MgOAc, 100 mM NH_4OAc. The cleavage reaction was initiated by addition of 0.001 µg/µl nuclease T1, 10^{-7} µg/µl ribonuclease A and 0.001 µg/µl nuclease V1 incubated at 37°C for 20 min (T1 and A), or 10 min (V1). For limited alkaline hydrolysis reaction, 10^4 Cerenkov cpm of end-labeled RNA (1/10 volume) were incubated with 2.5 µg of carrier tRNA in 0.2 M $NaHCO_3$–Na_2CO_3 pH 9 and 1 mM EDTA for 6.5 min at 90°C (9/10 volume).

The reactions were stopped by addition of two volumes of gel loading buffer, and products were resolved on 20% denaturing polyacrylamide gel. Gels were visualized by autoradiography.

Northern blot analysis

In order to facilitate the test of RNase P cleavage of HCV RNA in cells' cytoplasm, the $HCV_{299–408}$ sequence was inserted within the first cistron of plasmid pBIC previously described (26). This bicistronic vector contains the sequence of phage T7 promoter, the Chloramphenicol Acetyltransferase (CAT) coding sequence, the sequence of the Foot-and-Mouth Disease virus (FMDV) IRES and the luciferase coding sequence. The sequence of the $HCV_{299–408}$ (WT) was amplified by PCR and introduced in pBIC at a unique NcoI restriction site, located in the CAT coding sequence.

Transfection of 80–90% confluent BHK-21 monolayer was carried out using cationic liposomes 1 h after infection with the vaccinia virus VTF7-3, expressing T7 RNA polymerase in the cell cytoplasm (27).

Total RNA was extracted 16 h post-transfection, using the Tripure isolation Reagent (Roche). Time course expression assays visualized by northern analysis revealed that this was the optimal time of collection for newly transcribed bicistronic RNA with or without HCV RNA insert (data not shown). RNA (10 µg) was electrophoresed in a 1.5% agarose gel containing 2.2 M formaldehyde, 20 mM MOPS, 5 mM Na-Acetate and 1 mM EDTA. Electrophoresis buffer contained 20 mM MOPS, 5 mM Na-Acetate and 1 mM EDTA. Ethidium bromide was added directly to RNA samples in order to control the RNA input and the transfer efficiency. Transfer was performed by capillary blotting to a nylon membrane (Hybond-N+, Amersham Pharmacia Biotech) as indicated by the supplier.

Hybridization and detection was performed using the North2South Direct HRP Labelling and Detection kit (Pierce). The probes used were CAT 1–100 (100 bp), obtained by PCR from pBIC plasmid and $HCV_{299–408}$ (PCR product used to obtain the pBIC-HCV plasmid).

In vitro and *in vivo* IRES activity

In vitro translation was performed in 50% rabbit reticulocyte lysate, 10 mM HEPES–KOH (pH 7.5), 0.5 mM MgOAc, 100 mM NH_4OAc, 90 min at 30°C. Activity of IRES was quantified as the ratio of firefly luciferase on renilla luciferase using the Dual-Luciferase system (Promega).

Relative IRES activity was quantified *in vivo* as the expression of firefly luciferase normalized to that of renilla luciferase from bicistronic mRNAs in transfected cells with previously described full capacity to initiate translation from HCV IRES (28–30). Transfection of 80–90% confluent BHK-21 monolayers was carried out using cationic liposomes, 1 h after infection with the Vaccinia virus recombinant vTF7-3 expressing the T7 RNA polymerase (27). Extracts from 1–2 × 10^5 cells were prepared 20 h post-transfection in 100 µl of 50 mM Tris–HCl, pH 7.8, 120 mM NaCl, 0.5% NP40 (31).

Accession numbers

The nucleotide variant sequences for the hepatitis C virus 5′ non-coding region-core (5′ NCR-core) region described have been deposited in the GenBank database, accession numbers

AY576547–AY576603. Among these sequences, the four sequences from Patient 8 used for RNase P *in vitro* cleavage are AY576565 (Var 1), AY576574 (Var 2), AY576575 (Var 3) and AY576577 (Var 4). The WT and A368G sequences from HCV are, respectively, AY576552 and AY576555.

The nucleotide sequence of the reference 1b genotype HCV used in this study is available at the GenBank database under accession number S62220 (32).

RESULTS

Accessibility to RNase P *in vitro* is conserved despite HCV RNA primary sequence variation

In this study, we performed a detailed analysis of the viral quasispecies sequence composition of the 5′ NCR-core junction region (Figure 1), around the 5′ RNase P cleavage site. Changes in primary sequence may compromise structural organization required for optimal translation initiation, the most relevant function mapped to this region of the HCV genome. The characteristic quasispecies structure was found in a total of 155 sequences derived from eight patients. This includes a more frequent sequence in the population and a variable spectrum of mutants that was observed in all samples, as expected (1). A distinct consensus sequence was found in most of the samples analyzed, with the exception of viruses in three cases, which coincided with the 1b genotype standard sequence all along the IRES element and the beginning of the core-coding region. We subsequently compared the HCV mutant spectrum in the eight samples analyzed and found that a distinct, unique mutant spectrum accompanied each predominant sequence in the eight viral quasispecies. Notably, four variant sequences found in one of the samples studied presented mutations close to the RNase P cleavage site (Figure 3A), within the previously described tRNA-like motif (10,12). Because of the potential involvement of this structured region in internal translation initiation efficiency, we compared RNase P accessibility in parallel to the standard 1b genotype sequence. To this end, we used transcripts from cloned HCV PCR fragments, representing the predominant sequence as well as low frequency sequences from one infected patient (Patient 8) with mutations in the vicinity of the scissile bond (Var 1–4, Figure 3A). Cleavage with similar efficiency was consistently observed in triplicate experiments among natural variant sequences (Figure 3B), strongly suggesting that the RNA structural motif recognized by RNase P *in vitro* was a relevant feature of the HCV RNA. Decrease in the cleavage efficiency observed here in comparison with previous published results could be due to the use of different RNase P purified fractions, together with the use of a shorter HCV RNA substrate (10,12).

Isolation of a structural variant from HCV RNA quasispecies by an *in vitro* selection procedure

Taken together, the results in the previous section indicated that it would be laborious to find an altered RNA structure around the RNase P cleavage site by systematic testing of all the nucleotide mutants found in the viral quasispecies. *In vitro* selection of a variant carrying an altered RNA structure in the relevant motif was considered as a more direct approach.

RNase H was chosen as an 'easy-to-use' system for selecting potential HCV RNA conformation variants in the region close to human RNase P *in vitro* cleavage (Figures 1 and 2). We selected the sequences that were partially resistant to RNase H. DNA-mediated RNase H cleavage is sequence specific, but depends on previous hybridization of a DNA oligonucleotide to the target RNA, which in turn depends on RNA accessibility. We took the advantage offered by a previous study (25) that identified the HCV RNA fragment, encompassing nucleotides 339–361, as a relatively open region that allows efficient DNA-mediated RNase H cleavage in a reference genotype 1b sequence.

The HCV RNA natural population of variants from one of the eight patients [selected from a previous study because he presented one of the most heterogeneous HCV RNA quasispecies found in our laboratory, see (33): Table 1, patient 29] was subjected to *in vitro* selection using RNase H in the presence of a DNA oligonucleotide complementary to HCV RNA (positions 339–361), close to the HCV 5′ IRES RNase P cleavage site (Figures 1 and 2).

Selected HCV 2–418 RNA molecules were cloned and sequenced after two and four rounds of *in vitro* selection. Twenty clones were sequenced and compared to sequences cloned before the selection procedure, representing the serum HCV quasispecies (cycle 0). One point mutation, A368G, present in 10% of the sequences in serum, was enriched up to 50% of the sequences after four selection cycles. The predominant sequence in this patient's HCV RNA quasispecies is called wild-type (WT) all along this work and contains the mutations C204U and A214U when compared to the reference genotype 1b sequence. The A368G RNA sequence differs from the WT sequence only by the A368G mutation (see Figure 1).

A368G mutation decreases RNase H accessibility in $HCV_{2–418}$ RNA

To prove that the variant sequence being selected adopts a different RNA folding near the RNase P cleavage site, we performed a comparative analysis of the RNA sequences containing the mutation A368G or the WT RNA sequence with ribonucleases known to have structure-dependent activities.

RNase H. To confirm the phenotype of the *in vitro* selected sequence, a comparative kinetic RNase H cleavage experiment was performed on independently transcribed RNAs containing or not the selected mutation (A368G) (Figure 4). The kinetics of cleavage were clearly different and, as expected, it appeared that the mutant sequence was more resistant to RNase H cleavage than the WT sequence (Figure 4A, 3-fold effect). The relative resistance to cleavage by RNase H was observed in several experiments and was not due to a direct mismatch between the DNA oligonucleotide and RNA, since the mutation lies outside of the oligonucleotide hybridization site (Figure 1).

Additional RNase H kinetic experiments were performed to determine whether the A368G mutation induced other changes in RNA accessibility over the entire IRES than the one observed between nucleotides 339 and 361 (Figure 4B). Whereas HCV mutant RNA showed slightly reduced accessibility for RNase H cleavage when using a DNA oligonucleotide hybridizing to nucleotides 348–367 just upstream from the mutation site, DNA oligonucleotides encompassing

A

```
1b    (241)  gcgagacugc uagccgagua guguuggguc gcgaaaggcc uugugguacu
Var 1        ..a....... .......... .......... .......... ..........
Var 2        ..a....... .......... .......... .......... ..........
Var 3        .......... .......... .......... .......... ..........
Var 4        .......... .......... .......... .......... ..........

1b    (291)  gccugauagg gugcuugcga gugccccggg aggucucgua gaccgugcac
Var 1        .......... .......... .......... .......... ..........
Var 2        .......... .......... .......... .......... ..........
Var 3        .......... .......... .......... .......... ..........
Var 4        .......... .......... .......... .......... ..........

1b    (341)  cAUGAGCACG AAUCCUAAAC CUCAAAGAAA AACCAAACGU AACACCAACC
Var 1        .......... .......... .......... .......... ..........
Var 2        .......... .......... .......... .......... ....U.....
Var 3        .......... .......... .......... .......... ..........
Var 4        .......... .......... ........C. .......... ..........

1b    (391)  GCCGCCCACA GGACGUCAAG UUCCCGGG   (418)
Var 1        .U........ .......... ........
Var 2        .U........ .......... ........
Var 3        .U........ .......... ........
Var 4        .U........ .......... ........
```

B

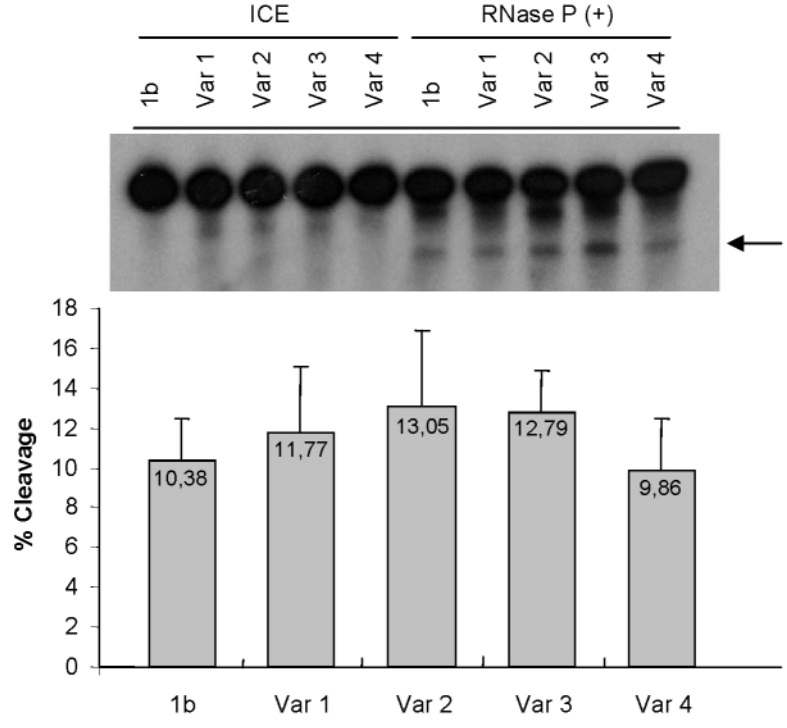

Figure 3. RNase P sensitivity of HCV RNA natural variants bearing substitutions in the RNase P cleavage region. (**A**) Sequence alignment of nucleotides 241–418 of cloned HCV variants. 1b represents the genotype 1b reference sequence and variants 1–4, four HCV variants isolated through cloning and sequencing of 2–418 region of HCV RNA (lower case, HCV 5′ NCR, upper case, HCV core coding region). RNase P cleavage site is underlined at positions 361–363. The position of the 3′ primer used for PCR and cloning is underlined (394–418). (**B**) Autoradiogram of RNase P *in vitro* cleavage assay of labeled 2–418 HCV RNAs. Variants 1–4 were incubated with RNase P, in parallel to 1b HCV RNA control, 1 h 30 min at 30°C. ICE indicates the input RNA, not incubated. Reaction products were fractionated in denaturing polyacrylamide–UREA gel electrophoresis followed of X-ray film exposure. The arrow indicates the larger cleavage product. Experiment was repeated as a triplicate and quantified with a Radioisotopic Image Analyser FLA-5000 (Fuji). The table below the autoradiogram indicates the average cleavage of each RNA determined as the ratio: products/products + uncleaved RNA.

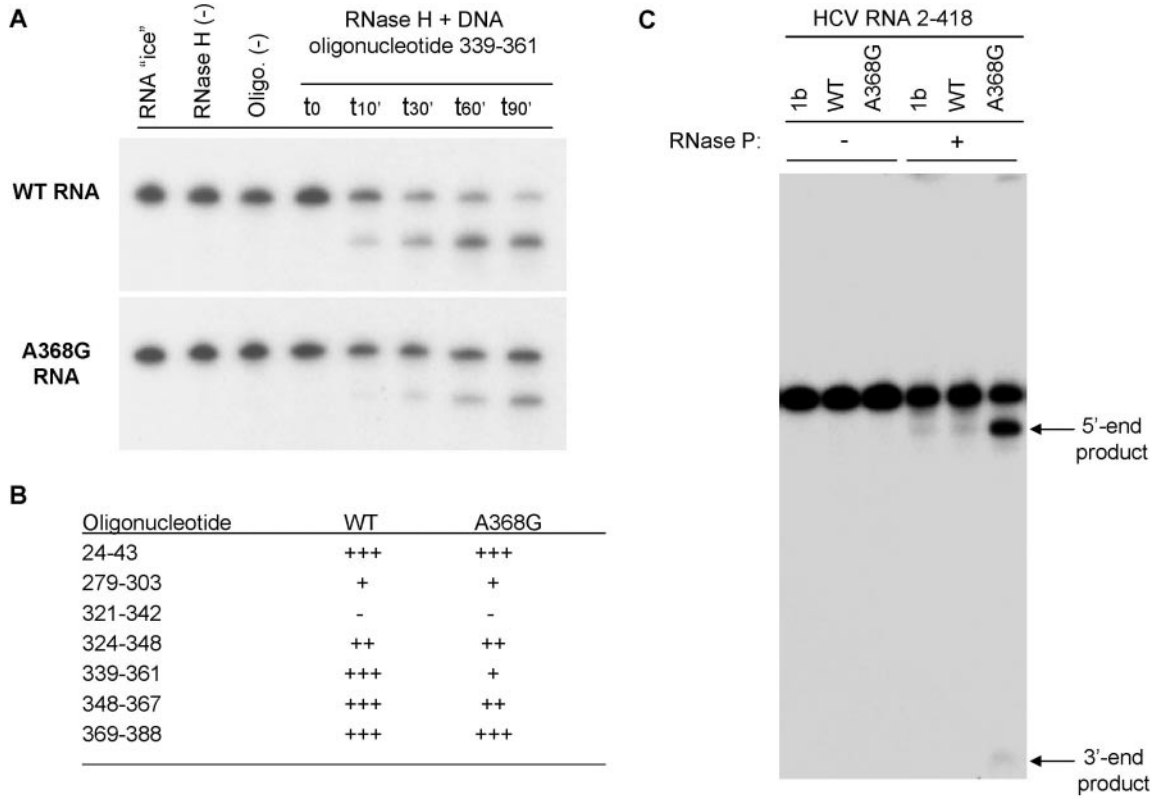

B

Oligonucleotide	WT	A368G
24-43	+++	+++
279-303	+	+
321-342	-	-
324-348	++	++
339-361	+++	+
348-367	+++	++
369-388	+++	+++

Figure 4. Enhanced accessibility to RNase P of the *in vitro* selected HCV RNA variant partially resistant to RNase H. (**A**) Time course DNA-mediated RNase H cleavage of the [α-^{32}P]GTP-labeled WT RNA compared to the A368G variant RNA (nucleotides 2–418), selected as indicated in Figure 2 using a DNA oligonucleotide complementary to nucleotides 339–361 of HCV RNA. Products were analyzed by denaturing PAGE (4%) and visualized by autoradiography. The kinetic study (0–90 min) shows the resistant phenotype associated with the mutant natural variant (estimated at a 3-fold effect). (**B**) Relative sensitivities of WT and A368G 2–418 HCV RNA to DNA-mediated RNase H cleavage. The oligonucleotide column indicates the positions where DNA oligonucleotides hybridize to RNA. +++: 75–100% of cleavage after 90 min, ++: 50–75%. +: 25–50%, −: 0–25%. (**C**) *In vitro* human RNase P cleavage of HCV 2–418 RNA. Lane 1b is the control genotype 1b HCV clone previously used in the laboratory to study RNase P cleavage (10) and represents here the cleavage efficiency and the product size control, lane WT is the HCV predominant sequence of the patient studied here, and lane A368G is the selected mutant sequence. RNase P (+) and (−) are, respectively, reactions with and without RNase P. Products were analyzed by denaturing PAGE (4%) and visualized by autoradiography. The position of the two 5′ and 3′ end RNase P cleavage products is indicated on the right.

nucleotides 24–43, 279–303, 321–342, 324–348 and 369–388 were seen to have the same cleavage kinetics in both WT and A368G HCV RNA. Thus, it seems that the A368G mutation induces a local structural reorganization affecting residues 339–367 of HCV RNA.

RNase P. To examine whether the structural changes between WT and A368G RNAs affected the tertiary RNA structure, which confers similarity to tRNA in the reference genotype 1b sequence, we tested in parallel the reference 1b, WT and A368G sequences with the human structure-dependent RNase P enzyme. This experiment revealed that A368G RNA is associated with strongly increased sensitivity to human RNase P (a more than 10-fold effect, Figure 4C), whereas WT and 1b RNAs are equally recognized by this enzyme.

HCV IRES A368G RNA presents an additional RNase P cleavage site as compared to WT RNA

Processing of mutant A368G by RNase P was not a simple case of increased cleavage efficiency to a variant RNA substrate. By analyzing cleavage products of shortened HCV substrates (nucleotides 291–418) on more concentrated acrylamide gels, we found two differentially migrating bands (L for Large and S for Short) in the variant RNA which can be interpreted as the result of an additional cleavage event (Figure 5A), not present in the WT RNA. Parallel electrophoresis of the WT and A368G RNA cleavage products showed a common pair of cleavage bands, both in position and intensity (79/80 and 62/61 nucleotide products) and a second pair of bands that were unique to the variant RNA (L and S). These two new bands showed only a slight difference in migration in the gel, but they were much more intense (Figure 5A).

Minimal HCV RNA substrate length necessary for RNase P cleavage

To determine the minimal substrate necessary for RNase P cleavage, WT and A368G HCV RNAs were sequentially shortened and treated with RNase P (Figure 5B). The shortest WT RNA processed by RNase P expanded from nucleotides 299 to 408 (110 nt, identical to the reference genotype 1b 299–408 sequence). However, cleavage efficiency was reduced and minor cleavage products began to appear as compared to

Figure 5

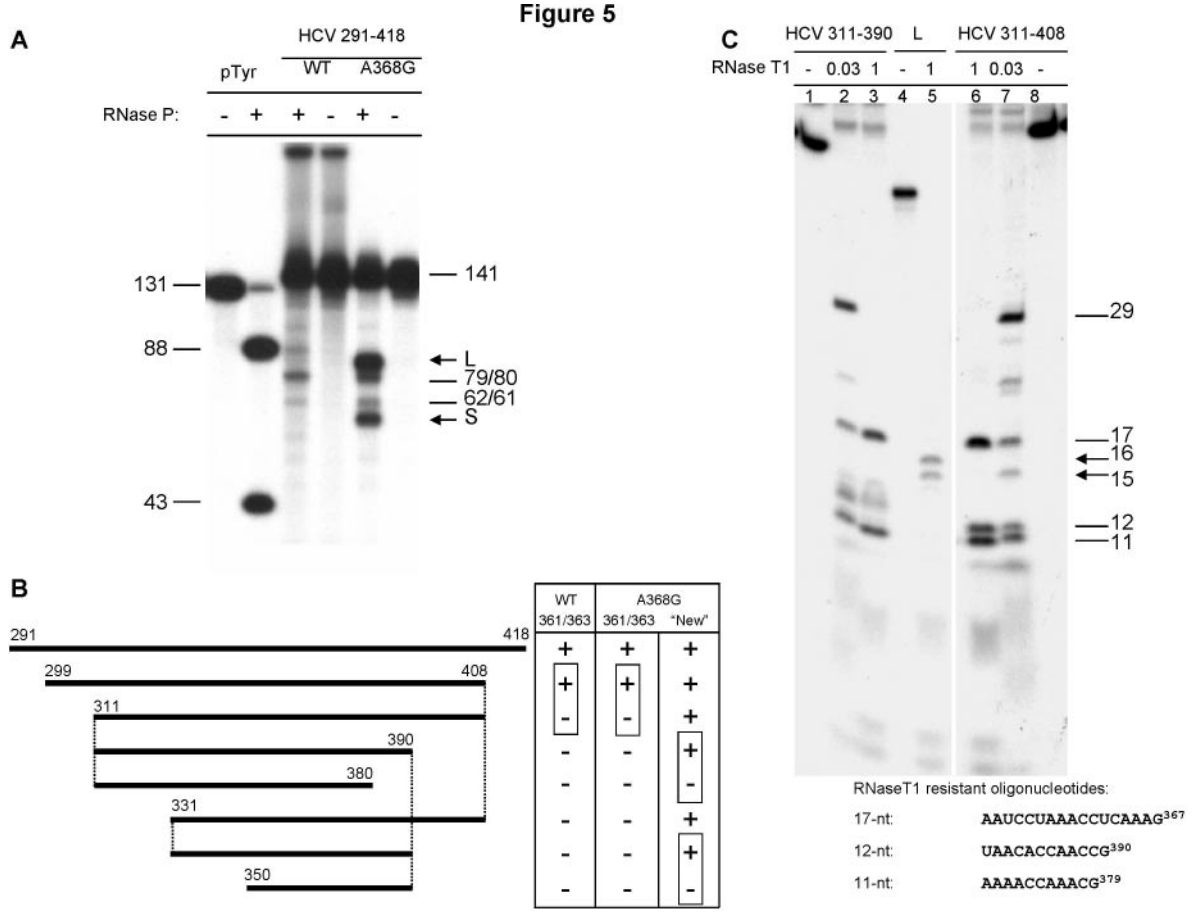

Figure 5. Identification of the minimal substrate for RNase P cleavage in the *in vitro* selected HCV RNA variant. (**A**) Comparison of the RNase P cleavage pattern of HCV WT and A368G. ^{32}P-labeled natural substrate for human RNase P (pTyr), HCV WT and A368G 291–418 RNAs were subjected (+) or not (−) to *in vitro* RNase P cleavage and analyzed on a 10% denaturing acrylamide gel. The arrows indicate the new cleavage products observed in A368G RNA, L (Large) and S (Short). Numbers indicate the length in nucleotides of RNA fragments. (**B**) Delimitation of the human RNase P minimal substrates in HCV WT or A368G RNA IRES. DNA templates were obtained by PCR, *in vitro* transcribed, and subjected to *in vitro* RNase P cleavage. Positions of RNase P cleavage are indicated as 361/363 for the previously described cleavage site, and as 'new' for the cleavage site described in this work. (**C**) Identification of the RNase P cleavage products. HCV mutant RNA 311–390 was treated with RNase P. Then, the 5′ end large cleavage product (L) was gel purified and subjected (lane 5) or not (lane 4) to total cleavage by RNase T1. Reaction products were analyzed on a 20% denaturing gel and compared to the HCV mutant RNA 311–390, also subjected to RNase T1 digestion (lanes 1, 2 and 3). RNase T1 cleavage fragments were run in parallel to those obtained at the same time from the 311–408 control RNA that allow the identification of the 11, 12 and 17 nt bands (lanes 6, 7 and 8). Numbers on the right indicate the length in nucleotides of RNA fragments. The table below the gel depicts the sequence of the 11, 12 and 17 nt HCV mutant RNA RNase T1 resistant oligonucleotides.

RNA fragments from nucleotides 291 to 418 (Figure 5A), probably indicating a loss of specific activity.

With regard to the A368G RNA, the shortest A368G RNA containing both RNase P cleavage sites [the first site previously described at position 361–363 (10) and the 'new' one] encompassed nucleotides 299–408, whereas the next construct containing nucleotides 311–408 only allowed for the 'new', and more effective, cleavage event. After decreasing the length of the substrate, specific cleavage still occurred in the fragment containing nucleotides 331–390, but not in the shorter RNA containing nucleotides 350–390 (Figure 5B).

To determine the position of the new cleavage site, we used an RNase T1 mapping strategy in a shortened A368G RNA fragment (nucleotides 311–390), which was shown to be substrate for human RNase P (see Figure 5B). Briefly, the largest RNase P cleavage product from 311–390 A368G RNA was gel purified and subjected to RNase T1 complete digestion. Digestion fragments were subsequently separated in 20% acrylamide gel. The longer RNase T1 cleavage fragments were identified as a doublet of 15 and 16 nt (Figure 5C), when compared to the electrophoretic mobility of the 11, 12 and 17 nt bands in the control lanes, obtained after total digestion of the 311–408 fragment. This showed that the major RNase P cleavage in mutant A368G RNA occurs between nucleotides 365 and 367, four nucleotides downstream from the first cleavage (see below, Figure 6C).

RNA secondary structure probing of the RNase P substrate present in HCV RNAs

Experiments involving partial digestion of HCV A368G and WT RNAs by single and double-strand RNA-specific nucleases were performed in order to characterize possible

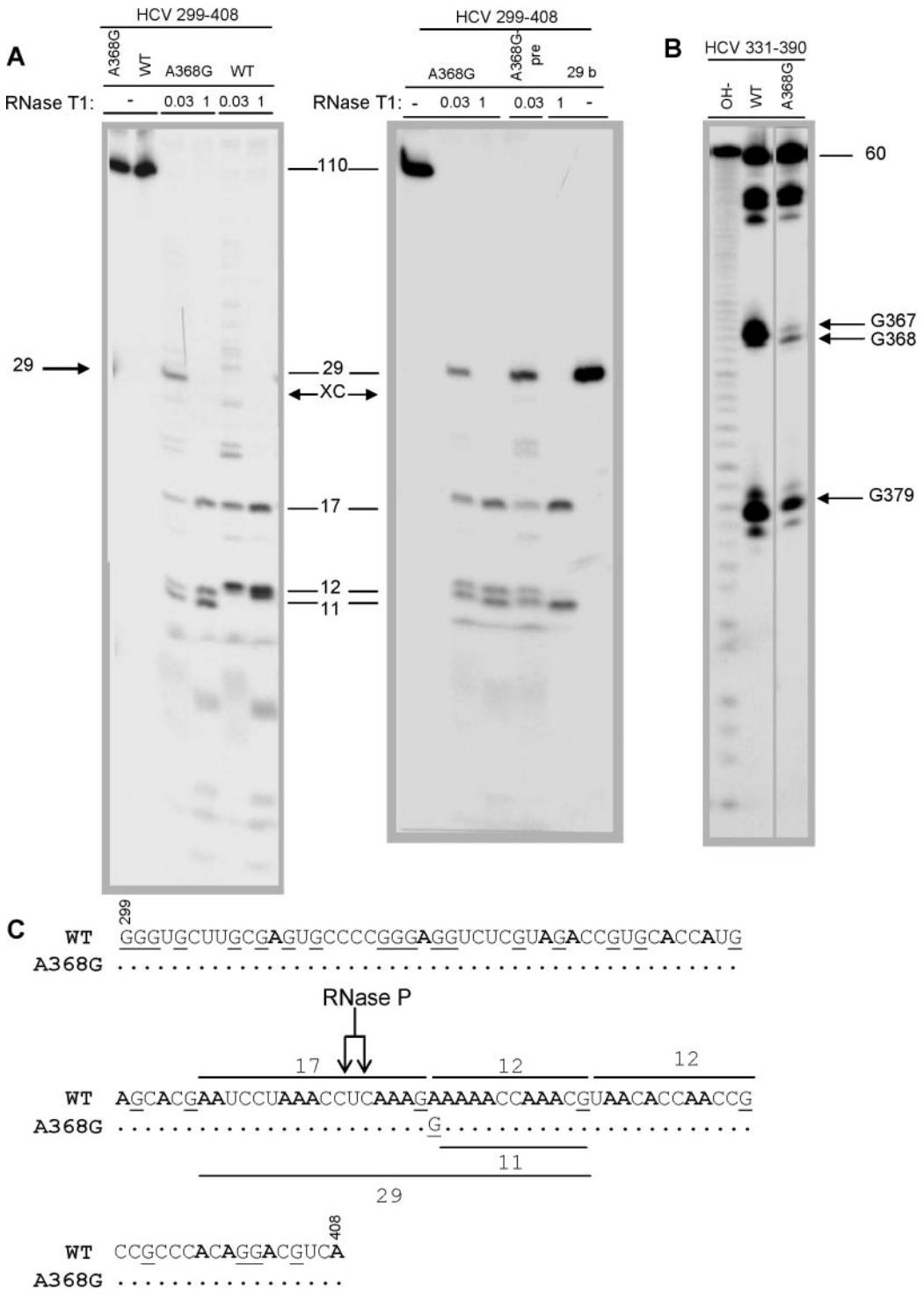

Figure 6. Enzymatic structural probing of the minimal fragment recognized by RNase P. (**A**) Comparison of RNase T1 cleavage pattern of WT and A368G uniformly ATP-labeled HCV RNAs (299–408). Left panel: A368G and WT RNA without RNase T1, or incubated with 0.03 or 1 μg/μl of RNase T1 during 20 min at 37°C in RNase P incubation buffer (10 mM HEPES–KOH, pH 7.5, 10 mM MgOAc, 100 mM NH_4OAc). Right panel: 'A368G': control reaction of mutant RNA incubated with 0.03 μg/μl or 1 μg/μl of RNase T1. 'A368G-pre': aliquot of HCV mutant 299–408 RNA cleaved by 0.03 μg/μl RNase T1, before gel purification of the 29 nt product. '29 b': gel-purified 29 nt product treated with or without 1 μg/μl RNase T1. Products were analyzed in denaturing PAGE (20%) and visualized by autoradiography. XC indicates xylene cyanol dye position (separates as a 28 nt fragment in 20% acrylamide gel); numbers in column indicate the length in nucleotides of RNA fragments. (**B**) RNase T1 partial digestion of 60 nt HCV 331–390 WT and A368G mutant RNAs. 3′ end-labeled RNAs were incubated with 0.001 μg/μl RNase T1, 20 min at 37°C and electrophoresed in a 20% acrylamide gel in parallel with one of the transcripts subjected to partial alkaline hydrolysis (OH-). (**C**) Diagram of RNase T1 cleavage products in WT and A368G HCV RNA sequences (299–408). The ^{32}P-labeled A residues appear in bold, G residues recognized by RNase T1 are underlined, and position of the described RNase P cleavage site in genotype 1b RNA is indicated. Numbers and lines indicate the largest predicted fragments. Position of the 29 nt product is also underlined.

differences in the RNA secondary structure. Two probing approaches were performed: (i) RNase T1 digestion of uniformly labeled transcripts and (ii) RNases T1, A or V1 partial digestion of end-labeled transcripts. To allow a better resolution of the reaction products in acrylamide gels, short 110 and 60 nt transcripts were used in (i) and (ii), respectively. The 110 nt RNA fragment (nt 299–408) is the minimal substrate for RNase P that is cleaved at both cleavage sites (361–363 and 365–367) and the 60 nt RNA fragment (nt 331–390) is the minimal substrate in the A368G RNA for RNase P cleavage at position 365–367 (see Figure 5B for details).

RNase T1 probing of transcripts bearing both RNase P sites: The reaction buffer, which contained 10 mM Mg^{2+} and was the same as that used in the RNase P assays, ensured that the RNA presented its magnesium-dependent structure (10,24). After RNase T1 partial cleavage of [α-^{32}P] ATP-labeled HCV RNA molecules, a 29 nt partial digest fragment was produced in A368G RNA, but not in WT RNA (Figure 6A, left panel). Same result was observed with [α-^{32}P]GTP-labeled RNAs using a wide range of RNase T1 concentration (data not shown). This partial digest fragment was gel purified and subjected to complete RNase T1 digestion (Figure 6A, right panel). The experiment showed that the 29 nt fragment separates into two visible fragments containing 11 and 17 nt. This result indicates that the 29 nt fragment is highly protected from cleavage by RNase T1 at positions G367 and G368 in A368G RNA (WT RNA contains only G367, Figure 6C). Residues G367 and G368 are probably engaged in Watson–Crick base pairing in A368G RNA, whereas G367 remains accessible to RNase T1 cleavage in the WT sequence.

RNases T1, A and V1 assays using end-labeled transcripts: WT and A368G 60 nt transcript were prepared, and subsequently labeled independently at the 5′ end with [α-^{32}P]GTP and guanylyl transferase ('cap' labeled) or at the 3′ end with ^{32}PpCp and T4 RNA ligase. Partial cleavage digestion products were run in parallel to the corresponding end-labeled transcript partially hydrolyzed by limited alkaline hydrolysis procedure. The result of the partial digestion of the 3′ end-labeled WT and A368G RNAs is shown in Figure 6B that clearly confirms the protection of residues G367 and G368 from RNase T1 cleavage in A368G RNA in the 60 nt molecule.

Figure 7 compiles the data of the positions protected from or accessible to cleavage by the nucleases, represented in the RNA structure for both WT and A368G 60 nt transcript predicted with the RNA structure 3.5 program (34). A stem–loop containing the AUG codon (nt 334–350) was predicted in both the WT and A368G sequences, in agreement with the nuclease mapping shown here and the HCV IRES secondary structure described up to now. The program also predicts the formation in the A368G RNA, but not in the WT RNA, of a stem–loop involving nucleotides 353–369. Enzymatic probing experiments, and especially experiments using the V1 nuclease, suggest that, in the WT sequence, a stem–loop could be formed implying the formation of a shorter stem between nucleotides 355–356 and 366–367 (which was thus

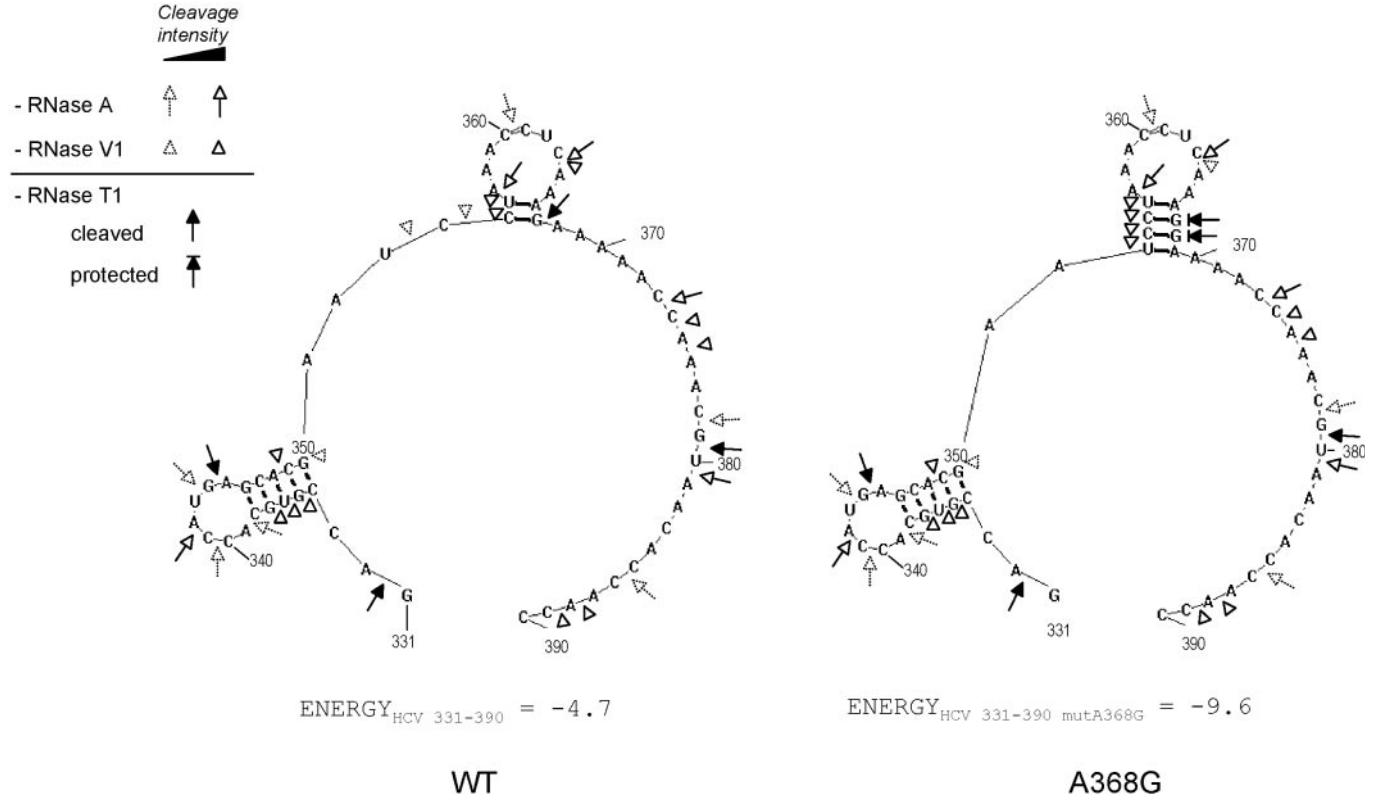

Figure 7. Summary of secondary structure probing of HCV 331–390 (WT and A368G) RNAs. Sensitivity to various RNases is indicated on the predicted RNA structure. $HCV_{331–390}$ WT structure was forced for base pairing between CU355–356 and AG366–367. $HCV_{331–390}$ A368G was predicted by RNA structure 3.5 program (34) (only one structure was predicted). Arrows indicate cleavages by single-strand-specific RNases T1 and A, whereas triangles show cleavage by double-strand-specific RNase V1. Nucleotide numbering is used as in Figure 1 (5′–3′ orientation).

represented in Figure 7). Additionally, some nuclease V1 cleavage events were located at positions 374–375 and 387–388 in an A-rich region actually sensitive to RNases A and T1 and predicted as single-strand. This could be explained by an RNA structure independent of Watson–Crick base pairing.

RNase P does not cleave HCV 5′ tRNA-like motif in the cytoplasm

Because RNase P is a nuclear enzyme and the virus replicates in the cytoplasm, it is unlikely that the RNase P processes the HCV RNA *in vivo*. Nevertheless, it cannot be discarded that a fraction of the enzyme is present in the cytoplasm, e.g. during biosynthesis or during transportation to mitochondria. The activity of RNase P in the cytoplasm would cleave HCV tRNA-like motif. We inserted the $HCV_{299–408}$ minimal substrate of the 1b reference sequence into a bicistronic construct (Figure 8A) and evaluated by northern analysis the presence of specific cleavage at the tRNA-like structure (Figure 8B). Two independent probes were used for hybridization, one corresponding to the vector CAT coding region (Figure 8B, left panel) and the other to the HCV insert (Figure 8B, right panel). Using the CAT probe, several bands were observed either in the control without insert (Figure 8B, lane pBic) or in the RNA containing the HCV insert (Figure 8B, lane HCV). The upper-most band below the 28S RNA marker, corresponds to the expected full-length transcript, the other bands could represent either premature stops in transcription or processing by endogenous nucleases. Examination of band pattern revealed that the only difference occurs in the mobility of the bands migrating below the 18S RNA marker that could be attributed to the HCV sequence insertion (110 nt). No new transcripts appeared in the HCV lane, discarding cleavage of HCV RNA by the endogenous RNase P. In the right panel of Figure 8B, hybridization with the specific HCV probe

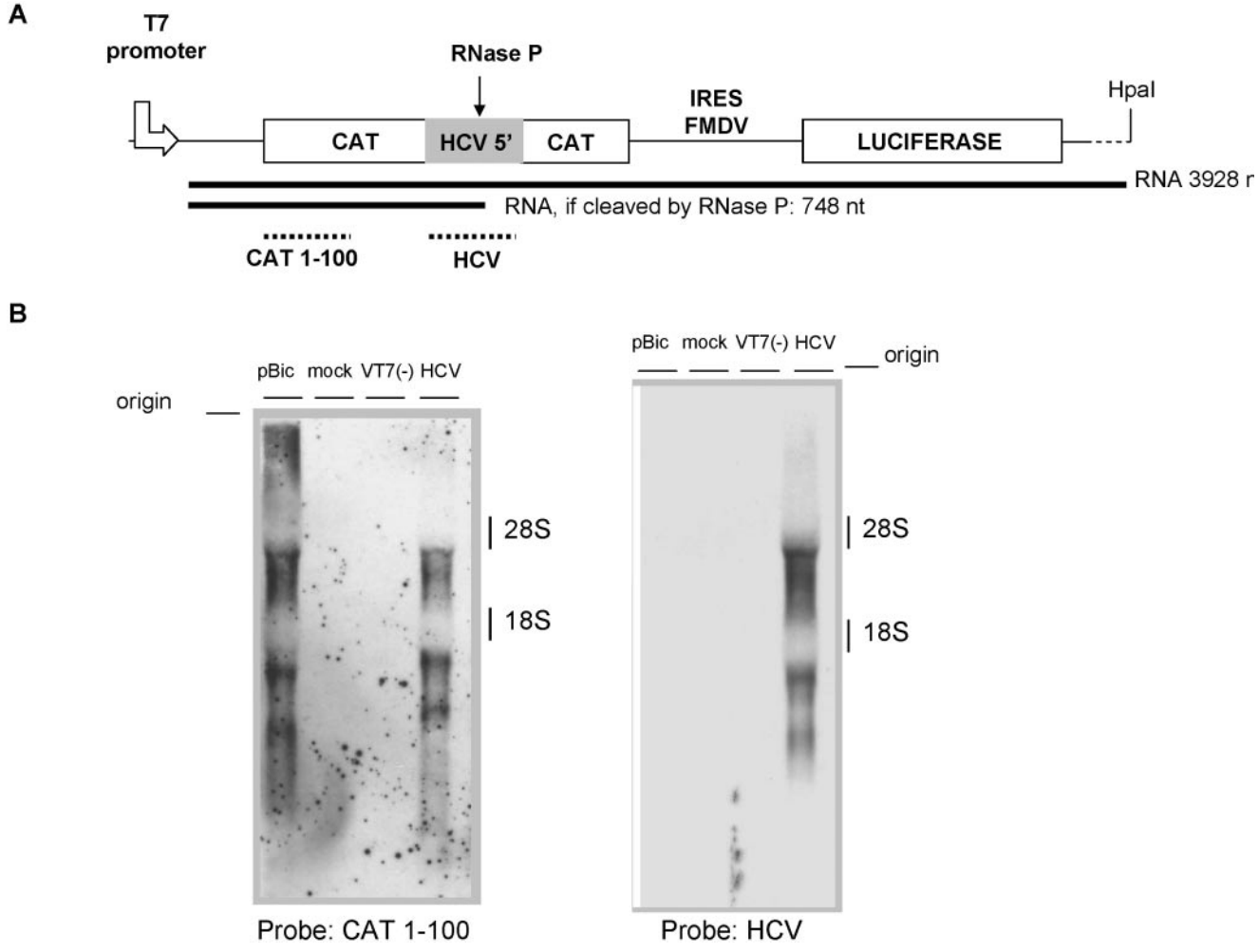

Figure 8. RNase P does not cleave HCV 5′ tRNA-like motif in the cytoplasm of transfected cells. (**A**) Schematic representation of the plasmid used to test the RNase P cleavage in the cytoplasm. HCV minimal domain (WT) cleaved *in vitro* by RNase P (HCV 299–408) was inserted in the coding sequence of CAT in the pBIC plasmid. The expected size of the RNA fragments, if cleaved by RNase P, is indicated. Positions of hybridization of CAT 1–100 and $HCV_{299–408}$ probes are indicated in dotted line (CAT 1–100 and HCV, respectively). (**B**) Northern blot analysis after transfection of BHK-21 cells with pBIC-HCV. BHK-21 cells were transfected with pBIC plasmids containing (HCV) or not (pBIC) the HCV target for RNase P *in vitro* cleavage. pBIC plasmids were linearized by HpaI before transfection. Controls were cells not transfected/infected (mock) or cells not infected [VT7(−)]. Total RNA was extracted from the cells at 16 h post-transfection, electrophoresed, transfered to a nylon membrane and hybridized with a pBIC-specific probe (CAT) or HCV-specific probe (HCV). The position of the ribosomal 28S and 18S RNA markers is indicated on the right.

confirmed the specificity of the detected transcripts and the absence of any new band relative to the pattern obtained with the CAT probe.

Translation efficiency of the WT and A368G sequences

The mutation of A368 to G in the ninth triplet of core coding sequence does not change the encoded amino acid (arginine). However, the effect of having two redundant signals that mimic tRNA structure in an IRES element was a novel feature, with unpredictable consequences for translational activity. Therefore, in order to assess whether the presence of a second stable stem–loop structure immediately downstream of the IRES region exerted an effect on the translational efficiency of this RNA, we tested the ability of both WT and A368G sequence to direct translation in both rabbit reticulocyte lysate (RRL, *in vitro*) and in cell culture (BHK-21 cells, *in vivo*). Bicistronic constructs have been proven useful to assay the HCV viral IRES variants in BHK-21 cells infected with the recombinant VT7F-3 vaccinia virus (28–30). Here, the bicistronic transcripts contained the Renilla luciferase gene as a first cap-dependent reporter, and the Firefly luciferase gene as a second HCV IRES-dependent reporter (Figure 9A).

In vitro translation experiments were performed, in presence of Mg^{2+} (0.5 mM), using RNAs previously transcribed and quantified. The presence of A368G mutation reduces the ability for the HCV IRES to direct translation (Figure 9B). In RRL, the Firefly luciferase expressed from mutated HCV IRES is 52.9% compared to expression from WT IRES without the mutation, and in BHK-21 transfected cells, 76.5%. Thus, the A368G mutation slightly reduces the IRES activity as compared to the wild-type sequence but does not prevent translation initiation, indicating that the variant RNA present in the viral quasispecies was being actively translated.

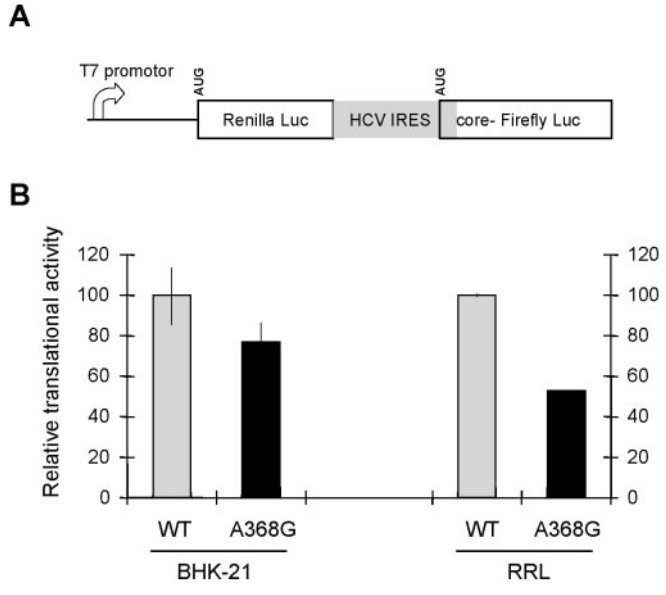

Figure 9. Effect of A368G mutation on IRES activity. (**A**) Diagram of the bicistronic plasmids used for the translation assays. The HCV RNA sequence is shown in a gray box (2–418). The first 26 amino acids of HCV core protein are fused in frame with the firefly luciferase. (**B**) Comparison of WT and A368G HCV IRES translation efficiency. IRES activity was assessed by measuring the ratio of Firefly Luciferase to Renilla Luciferase produced from plasmids transfected in BHK-21 cells or from *in vitro* transcribed RNA in rabbit reticulocyte lysate (RRL).

DISCUSSION

In this work, the minimal RNA fragment that confers accessibility to human RNase P has been found to be located between positions 299 and 408 of HCV consensus genome. After processing the minimal HCV tRNA-like motif, it was found that the longer portion (three-fifths of the substrate) coincides with part of domain IIIe, and domains IIIf and IV of the viral IRES, whereas the shorter portion (two-fifths of the substrate) expands 3′ outside the IRES region (Figure 1). The IIIe stem–loop does not appear to be necessary for RNase P cleavage; however, its participation in tRNA-like domain stabilization is not excluded, since the specificity and efficiency of cleavage are weakened in transcript 299–408 as compared to slightly longer RNA substrates 291–418. Moreover, the complete region that mimics the whole tRNA molecule may be larger than the region that is recognized by RNase P (i.e. the T and acceptor stems are enough for the RNase P recognition in its natural pre-tRNA substrate) (Figure 10A) (13).

Lack of a common mutation profile in the primary sequence covered by the tRNA-like motif among or within different viral quasispecies, and the fact that RNase P similarly recognizes variants carrying mutations close to the cleavage site suggest that the function exerted by this RNA motif is essential. Nevertheless, recognition of the tRNA-like domain was compatible with structural variations in the motif that allowed the formation of a second stem–loop near the cleavage site. From the HCV population of sequences (quasispecies) present in the serum of a single patient, we were able to isolate by an *in vitro* selection method, a natural HCV RNA structural variant containing a mutation (A368G) close to the AUG initiation codon that is present in 10% of the sequences in the serum quasispecies. This mutation seemed to stabilize an alternative RNA structure in comparison to the WT sequence, as measured by RNase H kinetics and accessibility to human RNase P.

It is worth noting that this variant RNA is translationally active, albeit with a slightly reduced efficiency either *in vitro* or in cell culture. As has been suggested before (6,7,9), the first nucleotides of the core coding sequence seem to have an important function in initiation of translation. Interestingly, the AUG downstream coding sequences of other viral IRESs, such as hepatitis A virus, GB virus B or Giardiavirus, have also been involved in IRES-dependent translation (35–37). However, conflicting results about the role played by this region is found in the literature (4,38,39). The presence of stable RNA structure downstream of the HCV AUG, different from the one present in natural HCV genome, appears detrimental to translation initiation (39). The findings of the present study suggest that the tRNA-like domain in HCV RNA IRES overlaps the AUG codon (nucleotide 342) including nucleotides from 299 to 408. The short hairpin found in the variant sequence with enhanced RNase P accessibility, appears to be a local internal RNA reorganization, not affecting either the upstream AUG-hairpin or the downstream A-rich core coding region. According to a previous report, the HCV core coding sequence, but not the core protein, is involved in IRES-dependent translation (39,40). Other works evidence

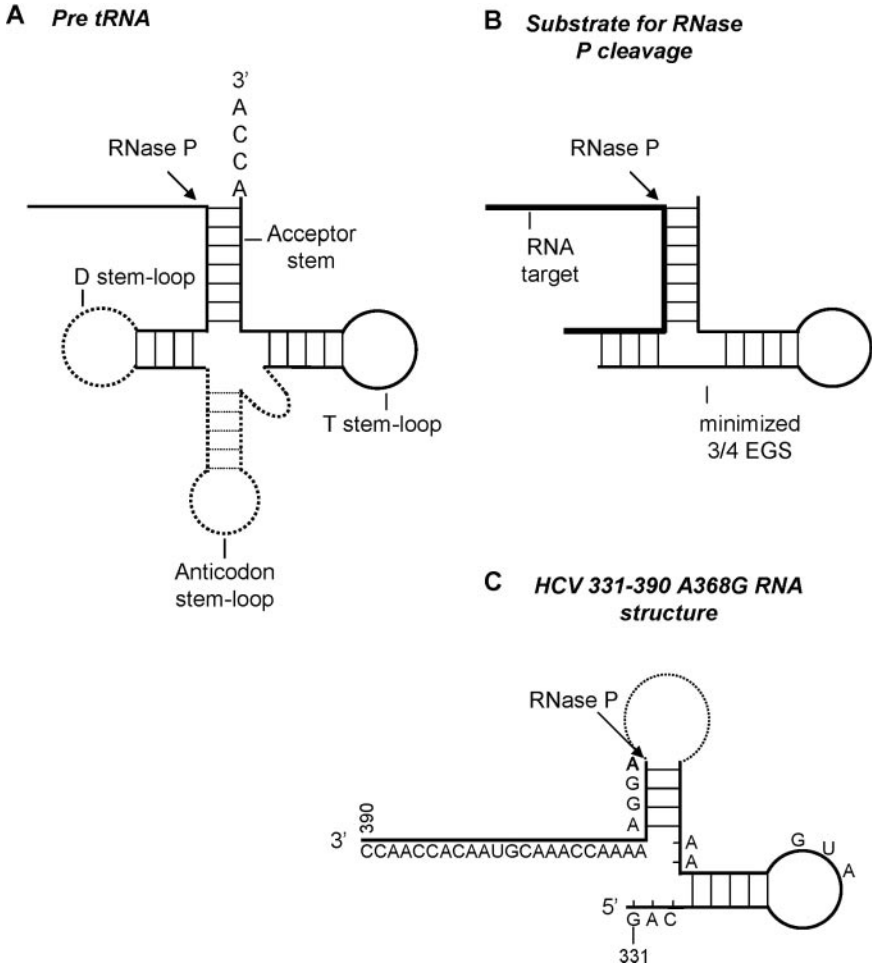

Figure 10. Comparison of HCV A368G RNA structure to that of human RNase P minimal substrate. (**A**) Diagram of pre-tRNA cloverleaf structure. An arrow indicates human RNase P cleavage site. Plain lines indicate the minimal structure necessary for RNase P recognition: acceptor stem, T stem–loop and D stem. (**B**) Diagram of a minimized external guide sequence (3/4 EGS) hybridized to a target RNA and recognized by human RNase P. (**C**) Representation of HCV A368G RNA structure (nucleotides 331–390, from Figure 8) to allow a comparison with a 3/4 EGS. The arrow indicates RNase P cleavage site in HCV A368G RNA.

long-range RNA–RNA interactions between the core coding sequence and the first bases of the IRES, which seem also detrimental to translation initiation (41,42). Thus, it seems that the core coding sequence is actually involved in numerous RNA secondary structures engaging various regions of the entire IRES that regulate translation initiation, allowing the virus to modulate its translational activity.

According to the data obtained by RNase P *in vitro* cleavage, we found that RNase P was recognizing a shorter 60 nt RNA motif in the mutant sequence, internal to the minimal fragment required for the predominant type. This represents a natural variant with an embedded tRNA-like motif, in a 'Russian-doll'-like conformation. Mapping the internal motif with a battery of RNases indicates the probable formation in the mutant of a stable stem–loop two nucleotides downstream of the AUG containing stem–loop (Figure 7). We compared this new RNase P 60 nt substrate with well-known substrates of RNase P. The transcript containing the two stem–loop structures in the A368G RNA (predicted *in silico* and demonstrated biochemically in this work) can be compared to the minimal structure required for RNase P recognition in its natural tRNA precursor substrate (Figure 10B and C). A 30 nt external guide sequence (EGS) that is, a minimized 3/4 EGS, seems sufficient to guide RNase P cleavage to an RNA target (13,43,44). The 30 nt are distributed as a first stem formed by 7 nt complementary to the target RNA, followed by the original T-stem–loop of the tRNA precursor and 4 nt complementary to the RNA target, which forms a second stem similar to the pre-tRNA stem of the D stem–loop (Figure 10A and B). The structure predicted for the minimum 60 nt HCV A368G RNA could resemble the EGS structure because of the presence of a loop, the total length of stem and stem–loop (9 nt separated by two unpaired nucleotides), and the RNase P cleavage position (Figure 10, compare B and C). Nevertheless, the HCV loop sequence is very different from the well-conserved pre-tRNA stem–loop. Additionally, the 4 nt forming the second stem in a typical EGS are lacking in the HCV structure. Thus, the tRNA-like motif present in 331–390 HCV A368G RNA seems to be a new type of substrate for RNase P with a structure slightly different from the well-known minimized 3/4 EGS.

It appears that none of the nucleotide preceding stem–loop IV, which contains the AUG, are necessary for efficient and specific RNase P cleavage in the tRNA-like domain stabilized

by the A368G mutation. Thus, this novel tRNA-like structure seems to be independent of stem–loop IIIe and of the well-described pseudoknot structure, both of which would have been good candidates for stabilization of a tRNA-like domain. The 'mutant' tRNA-like domain appears as a 'core' domain of 60 nt composed of two stem–loops separated by two unpaired nucleotide and followed by a stretch of 21 nt, that includes the A-rich region, without a predictable secondary structure (Figure 7). Since these 21 downstream nucleotides are necessary for RNase P to cleave, they are likely to be involved in RNase P recognition (39,45). Nevertheless, from the experiments performed here, it is difficult to explain why the variant is a better substrate than the WT molecule.

We should note that the tRNA-like motif described here seems to have a reverse orientation when compared to the natural pre-tRNA substrate, where all the structural determinants for RNase P recognition are located downstream from the cleavage site (Figure 10A). This result led support to a previous observation where after detecting stretches of sequence conservation in the predicted RNA secondary structure of HCV and pestiviruses IRESes, Lyons and Robertson proposed that most of the portion constituting the tRNA-like motif detected in IRES of these viruses would precede the cleavage site (12). We also observed that endogenous RNase P did not cleave HCV RNA in transfected cells, which suggests that RNase P is not involved in HCV cytoplasmic viral cycle. We therefore favor the idea that other cellular factors involved in tRNA metabolism may recognize the tRNA-like structure in HCV RNA. Taken together, all these observations suggest that the major part of the tRNA-like structure resides within the IRES and probably participates in its function in the manner of an RNA signal, as in other molecular systems where tRNA-like structures are found (46).

The structure of viral RNA has been interpreted as an element that imposes limitations on RNA genome evolution. To off-balance this situation, viral IRESs present compensatory mutations to preserve the higher order structures and their binding to the ribosome (47). In this study, we recognize within the viral quasispecies the presence of different conformations in a motif that is probably involved in IRES function. In agreement with this, the presence of this alternative secondary structure does not prevent the IRES from directing translation (see Figure 9). In this regard, the results shown here indicate that having two signals for RNase P recognition, i.e. two tRNA-like motifs, is compatible with ribosome recognition but is not better than one signal for IRES activity. Thus, we have an experimentally proven example of genotype–phenotype relationship in RNA that might accommodate most of the evolutionary implications applying to viral quasispecies (48). The results presented in this work illustrate the diversity that an RNA signal may adopt as a given entity in viral RNAs.

ACKNOWLEDGEMENTS

We are grateful to María Martell for critical reading of the manuscript, to Hugh Robertson for helpful discussions and advice, and to Celine Cavallo for the English revision of the manuscript. This work was supported in part by the BIO2000-347, FISS 01/1351, BIO2004-06114 and FIPSE 36293/02 grants from the Spanish Comisión Interministerial de Ciencia y Tecnología and the Fondo de Investigaciones Sanitarias, and BMC2002-00983 to E.M.S. M.P. was supported by grants from l'Association pour la Recherche sur le Cancer (ARC), the European Commission (Marie Curie postdoctoral fellowship QLK2-CT-2000-51150) and the Institut de Recerca del Hospital Vall d'Hebron (IRHVH). Funding to pay the open access publication charges for this article was provided by BIO2004-06114.

REFERENCES

1. Martell,M., Esteban,J.I., Quer,J., Genesca,J., Weiner,A., Esteban,R., Guardia,J. and Gomez,J. (1992) Hepatitis C virus (HCV) circulates as a population of different but closely related genomes: quasispecies nature of HCV genome distribution. *J. Virol.*, **66**, 3225–3229.
2. Domingo,E. and Holland,J.J. (1994) Mutation rates and rapid evolution of RNA viruses. In Morse,S.S. (ed.), *Evolutionary Biology of Viruses*. Raven Press, New York, pp. 161–184.
3. Schuster,P. (1997) Genotypes with phenotypes: adventures in an RNA toy world. *Biophys. Chem.*, **66**, 75–110.
4. Tsukiyama-Kohara,K., Iizuka,N., Kohara,M. and Nomoto,A. (1992) Internal ribosome entry site within hepatitis C virus RNA. *J. Virol.*, **66**, 1476–1483.
5. Honda,M., Ping,L.H., Rijnbrand,R.C., Amphlett,E., Clarke,B., Rowlands,D. and Lemon,S.M. (1996) Structural requirements for initiation of translation by internal ribosome entry within genome-length hepatitis C virus RNA. *Virology*, **222**, 31–42.
6. Reynolds,J.E., Kaminski,A., Kettinen,H.J., Grace,K., Clarke,B.E., Carroll,A.R., Rowlands,D.J. and Jackson,R.J. (1995) Unique features of internal initiation of hepatitis C virus RNA translation. *EMBO J.*, **14**, 6010–6020.
7. Reynolds,J.E., Kaminski,A., Carroll,A.R., Clarke,B.E., Rowlands,D.J. and Jackson,R.J. (1996) Internal initiation of translation of hepatitis C virus RNA: the ribosome entry site is at the authentic initiation codon. *RNA*, **2**, 867–878.
8. Rijnbrand,R., Bredenbeek,P., van der Straaten,T., Whetter,L., Inchauspe,G., Lemon,S. and Spaan,W. (1995) Almost the entire 5′ non-translated region of hepatitis C virus is required for cap-independent translation. *FEBS Lett.*, **365**, 115–119.
9. Fletcher,S.R., Ali,I.K., Kaminski,A., Digard,P. and Jackson,R.J. (2002) The influence of viral coding sequences on pestivirus IRES activity reveals further parallels with translation initiation in prokaryotes. *RNA*, **8**, 1558–1571.
10. Nadal,A., Martell,M., Lytle,J.R., Lyons,A.J., Robertson,H.D., Cabot,B., Esteban,J.I., Esteban,R., Guardia,J. and Gomez,J. (2002) Specific cleavage of Hepatitis C virus RNA genome by human RNase P. *J. Biol. Chem.*, **277**, 30606–30613.
11. Sabariegos,R., Nadal,A., Beguiristain,N., Piron,M. and Gomez,J. (2004) Catalytic RNase P RNA from *Synechocystis sp*. cleaves the hepatitis C virus RNA near the AUG start codon. *FEBS Lett.*, **577**, 517–522.
12. Lyons,A.J. and Robertson,H.D. (2003) Detection of tRNA-like structure through RNase P cleavage of viral internal ribosome entry site RNAs near the AUG start triplet. *J. Biol. Chem.*, **278**, 26844–26850.
13. Gopalan,V., Vioque,A. and Altman,S. (2002) RNase P: variations and uses. *J. Biol. Chem.*, **277**, 6759–6762.
14. Baumstark,T. and Ahlquist,P. (2001) The brome mosaic virus RNA3 intergenic replication enhancer folds to mimic a tRNA TpsiC-stem loop and is modified *in vivo*. *RNA*, **11**, 1652–1670.
15. Guerrier-Takada,C., van Belkum,A., Pleij,C.W. and Altman,S. (1988) Novel reactions of RNAase P with a tRNA-like structure in turnip yellow mosaic virus RNA. *Cell*, **53**, 267–272.
16. Joshi,S., Chapeville,F. and Haenni,A.L. (1982) Length requirement for tRNA-specific enzymes and cleavage specificity at the 3′ end of turnip yellow mosaic virus RNA. *Nucleic Acids Res.*, **10**, 1947–1962.
17. Komine,Y., Kitabatake,M., Yokogawa,T., Nishikawa,K. and Inokuchi,H. (1994) A tRNA-like structure is present in 10Sa RNA, a small stable RNA from *E.coli*. *Proc. Natl Acad. Sci. USA.*, **91**, 9923–9227.
18. Peck-Miller,K. and Altman,S. (1991) Kinetics of the processing of the precursor to 4.5S RNA, a naturally occuring substrate for RNase P from *E. coli*. *J. Mol. Biol.*, **221**, 1–5.
19. Kieft,J.S., Zhou,K., Jubin,R. and Doudna,J.A. (2001) Mechanism of ribosome recruitment by hepatitis C IRES RNA. *RNA*, **7**, 194–206.

20. Pestova,T.V., Shatsky,I.N., Fletcher,S.P., Jackson,R.J. and Hellen,C.U. (1998) A prokaryotic-like mode of cytoplasmic eukaryotic ribosome binding to the initiation codon during internal translation initiation of hepatitis C and classical swine fever virus RNAs. *Genes Dev.*, **12**, 67–83.
21. Kolupaeva,V.G., Pestova,T.V. and Hellen,C.U. (2000) An enzymatic footprinting analysis of the interaction of 40S ribosomal subunits with the internal ribosomal entry site of hepatitis C virus. *J. Virol.*, **74**, 6242–6250.
22. Lytle,J.R., Wu,L. and Robertson,H.D. (2001) The ribosome binding site of Hepatitis C virus mRNA. *J. Virol.*, **75**, 7629–7636.
23. Lytle,J.R., Wu,L. and Robertson,H.D. (2002) Domains on the hepatitis C virus internal ribosome entry site for 40S subunit binding. *RNA*, **8**, 1045–1055.
24. Kieft,J.S., Zhou,K., Jubin,R., Murray,M.G., Lau,J.Y.N. and Doudna,J.A. (1999) The Hepatitis C virus internal ribosome entry site adopts an ion-dependent tertiary fold. *J. Mol. Biol.*, **292**, 513–529.
25. Lyons,A.J., Lytle,J.R., Gómez,J. and Robertson,H.D. (2001) Hepatitis C virus internal ribosome entry site RNA contains a tertiary structural element in a functional domain of stem–loop II. *Nucleic Acids Res.*, **29**, 2535–2541.
26. Martinez-Salas,E., Saiz,J.C., Davila,M., Belsham,G.J. and Domingo,E. (1993) A single nucleotide substitution in the internal ribosome entry site of foot-and-mouth disease virus leads to enhanced cap-independent translation in vivo. *J. Virol.*, **67**, 3748–3755.
27. Fuerst,T.R., Niles,E.G., Studier,F.W. and Moss,B. (1986) Eukaryotic transient-expression system based on recombinant vaccinia virus that synthesizes bacteriophage T7 RNA polymerase. *Proc. Natl Acad. Sci. USA*, **83**, 8122–8126.
28. Borman,A.M., Le Mercier,P., Girard,M. and Kean,K.M. (1997) Comparison of picornaviral IRES-driven internal initiation of translation in cultured cells of different origins. *Nucleic Acids Res.*, **25**, 925–932.
29. López de Quinto, Lafuente,E. and Martinez-Salas,E. (2001) IRES interaction with translation initiation factors: functional characterization of novel RNA contacts with eIF3, eIF4B, and eIF4GII. *RNA*, **7**, 1213–1226.
30. Saiz,J.C., López de Quinto,S., Ibarrola,N., López-Labrador,F.X., Sánchez-Tapias,J.M., Rodés,J. and Martínez-Salas,E. (1999) Internal initiation of translation efficiency in different hepatitis C genotypes isolated from interferon treated patients. *Arch. Virol.*, **144**, 215–229.
31. López de Quinto and Martinez-Salas,E. (1997) Conserved structural motifs located in distal loops of aphthovirus internal ribosome entry site domain 3 are required for internal initiation of translation. *J. Virol.*, **71**, 4171–4175.
32. Hayashi,N., Higashi,H., Kaminaka,K., Sugimoto,H., Esumi,M., Komatsu,K., Hayashi,K., Sugitani,M., Suzuki,K. and Tadao,O. (1993) Molecular cloning and heterogeneity of the human hepatitis C virus (HCV) genome. *J. Hepatol.*, **17**, S94–S107.
33. Cabot,B., Martell,M., Esteban,J.I., Sauleda,S., Otero,T., Esteban,R., Guardia,J. and Gomez,J. (2000) Nucleotide and amino acid complexity of hepatitis C virus quasispecies in serum and liver. *J. Virol.*, **74**, 805–811.
34. Mathews,D.H., Sabina,J., Zuker,M. and Turner,D.H. (1999) Expanded sequence dependence of thermodynamic parameters improves prediction of RNA secondary structure. *J. Mol. Biol.*, **288**, 911–940.
35. Garlapati,S. and Wang,C.C. (2002) Identification of an essential pseudoknot in the putative downstream internal ribosome entry site in giardiavirus transcript. *RNA*, **8**, 601–611.
36. Graff,J. and Ehrenfeld,E. (1998) Coding sequences enhance internal initiation of translation by hepatitis A virus RNA *in vitro*. *J. Virol.*, **72**, 3571–3577.
37. Pizzuti,M., De Tomassi,A. and Traboni,C. (2003) Replication and IRES-dependent translation are both affected by core coding sequences in subgenomic GB virus B replicons. *J. Virol.*, **77**, 7502–7509.
38. Fukushi,S., Katayama,K., Kurihara,C., Ishiyama,N., Hoshino,F.B., Ando,T. and Oya,A. (1994) Complete 5′ noncoding region is necessary for the efficient internal initiation of hepatitis C virus RNA. *Biochem. Biophys. Res. Commun.*, **199**, 425–432.
39. Rijnbrand,R., Bredenbeek,P.J., Haasnoot,P.C., Kieft,J.S., Spaan,W.J. and Lemon,S.M. (2001) The influence of downstream protein-coding sequence on internal ribosome entry on hepatitis C virus and other flavivirus RNAs. *RNA*, **7**, 585–597.
40. Wang,T.H., Rijnbrand,R.C.A. and Lemon,S.M. (2000) Core protein-coding sequence, but not core protein, modulates the efficiency of cap-independent translation directed by the internal ribosome entry site of hepatitis C virus. *J. Virol.*, **74**, 11347–11358.
41. Honda,M., Beard,M.R., Ping,L.H. and Lemon,S.M. (1999) A phylogenetically conserved stem–loop structure at the 5′ border of the internal ribosome entry site of hepatitis C virus is required for cap-independent viral translation. *J. Virol.*, **73**, 1165–1174.
42. Kim,Y.K., Lee,S.H., Kim,C.S., Seol,S.K. and Jang,S.K. (2003) Long-range RNA–RNA interaction between the 5′ nontranslated region and the core-coding sequences of hepatitis C virus modulates the IRES-dependent translation. *RNA*, **9**, 599–606.
43. Yuan,Y. and Altman,S. (1994) Selection of guide sequences that direct efficient cleavage of mRNA by human ribonuclease P. *Science*, **263**, 1269–1273.
44. Yuan,Y., Hwang,E.S. and Altman,S. (1992) Targeted cleavage of mRNA by human RNase P. *Proc. Natl Acad. Sci. USA*, **89**, 8006–8010.
45. Honda,M., Brown,E.A. and Lemon,S.M. (1996) Stability of a stem–loop involving the initiator AUG controls the efficiency of internal initiation of translation on hepatitis C virus RNA. *RNA*, **2**, 955–968.
46. Springer,M., Portier,C. and Grunberg-Manago,M. (1998) RNA mimicry in the translational apparatus. In Simons,R.W. (ed.), *RNA Structure and Function.* Cold Spring Harbor Laboratory Press, Cold Spring Harbor, NY, pp. 377–413.
47. Martinez-Salas,E., Regalado,M.P. and Domingo,E. (1996) Identification of an essential region for internal initiation of translation in the aphthovirus internal ribosome entry site and implications for viral evolution. *J. Virol.*, **70**, 992–998.
48. Domingo,E. and Holland,J.J. (1997) RNA virus mutations and fitness for survival. *Annu. Rev. Microbiol.*, **51**, 151–178.